

Conductivity from magnetic polarons to variable-range hopping in $\text{FeCr}_{2-x}\text{Al}_x\text{S}_4$

Zhaorong Yang,* Shun Tan, and Yuheng Zhang

Structure Research Laboratory, University of Science and Technology of China, Academia Sinica,
and National High Magnetic Field Laboratory, Hefei, Anhui 230026, People's Republic of China

(Received 13 October 2000; revised manuscript received 29 January 2001; published 7 June 2001)

In this paper, the magnetic and transport properties of $\text{FeCr}_{2-x}\text{Al}_x\text{S}_4$ ($0 < x \leq 1.0$) are studied. The experimental results of infrared spectra, magnetization, and electron spin resonance indicate that the substitution of Al for Cr ions induces both Coulomb and magnetic-potential fluctuations to the system, which favor the carrier localization. With increasing Al content, the magnetic transition weakens and broadens, the conduction behavior transits from magnetic-polaron transport to the variable-range hopping process, and the colossal magnetoresistance effect decreases and disappears at last.

DOI: 10.1103/PhysRevB.64.024401

PACS number(s): 75.70.Pa

I. INTRODUCTION

Hole-doped manganite perovskites have become the focus of scientific and technological interest in the past several years because they exhibit the colossal magnetoresistance (CMR) effects.¹⁻³ Within the framework of the double-exchange model and the Jahn-Teller (JT) polarons, the magnetic and transport properties in these compounds can be explained qualitatively.^{4,5} In addition, several other factors are also suspected to influence the conduction behavior, such as the presence of magnetic disorder and the intrinsic variations in the Coulomb potential due to the presence of A^{3+} and A^{2+} ions in the lattice.^{6,7}

FeCr_2S_4 is another kind of CMR material, however, it has neither heterovalence nor the JT polaron,^{8,9} whose magnetoresistance mechanism was initially speculated to arise from scattering between carriers and critical fluctuations; the conduction in FeCr_2S_4 was believed to originate from the Fe^{2+} narrow band.¹⁰ Recent works have suggested that the carrier exists in the form of a magnetic polaron in the conduction process at temperatures above T_c .¹¹ In addition, FeCr_2S_4 is ferrimagnetic,^{12,13} both Fe sublattice and Cr sublattice are ferromagnetic, while between two sublattices the spins are in antiferromagnetic arrangement, this kind of magnetic arrangement will inevitably influence the conductivity and determine the CMR effect. In this paper, we design a series of samples with Al substituting for Cr ($\text{FeCr}_{2-x}\text{Al}_x\text{S}_4$, $0 < x \leq 1.0$) through which the influence of disorder-induced localization on the magnetic-polaron transport behavior has been studied. The reason we chose Al to substitute for Cr is that the radius of Al^{3+} ions is much smaller than that of Cr^{3+} ions, thus Al substituting more easily causes the fluctuation of Coulomb potential.

Our results indicate that with increasing Al content, the resistivity increases and the conduction behavior transits from magnetic-polaron transport to the variable-range hopping (VRH) process. It is believed that the substitution of Al for Cr induces both Coulomb- and magnetic-potential fluctuations, which cause the carrier localization. When the localization length is much small, the transport behavior is mainly determined by the VRH process. In addition, the magnetic transition weakens and broadens. As a consequence, the magnetoresistance effect decreases and disappears at last.

II. EXPERIMENT

The polycrystalline samples of $\text{FeCr}_{2-x}\text{Al}_x\text{S}_4$ ($0 < x \leq 1.0$) were prepared by the standard solid-state synthesis method.⁸ High-purity powders of iron (99.9%), chromium (99.9%), aluminum (99.9%), and sulphur (99.9%) were mixed uniformly in a 6 g batch according to the stoichiometric ratio and sealed into evacuated quartz tubes. The tubes were slowly heated from 450 °C to 850 °C with a step of 50 °C over a period of 1 week. The initially sintered samples were ground and pressed into round or square-shaped pellets (10 mm diameter, 4 mm thick or $20 \times 5 \times 4 \text{ mm}^3$). The pellets were resealed in evacuated quartz tubes and heated up to 950 °C and then left at the temperature for 3 days.

The x-ray power diffraction (XRD) data were collected on a rotating anode x-ray diffractometer, type MXP 18AHF, with graphite-monochromatized $\text{Cu } K\alpha$ radiation. The measurements of infrared transmission spectra were carried out with powder samples in the frequency range from 4000 to 350 cm^{-1} . The magnetization M in the temperature range from 4.2 to 400 K were measured using a M-9300 vibrating sample magnetometer under 0.5 T for $x \leq 0.7$ and 0.005 T for $x \geq 0.8$. The electron spin resonance (ESR) spectra were recorded on the powder sample in a Bruker ER200D spectrometer at 9.4 GHz. The resistivity measurements were performed using a standard four-probe method in the temperature range from 4.2 to 300 K under an applied field of 0 and 5 T.

III. EXPERIMENTAL RESULTS AND DISCUSSION

A. Pure phase with spinel structure

Structure and phase purity of $\text{FeCr}_{2-x}\text{Al}_x\text{S}_4$ ($0 < x \leq 1.0$) were examined by XRD measurements, which reveal that all samples are single phased with spinel structure. The lattice parameter for each sample was computed by means of a weighted least-squares fitting, which is shown in Table I. On substitution of Cr by Al, no structure change has been observed.

B. Fluctuation of Coulomb potential and magnetic inhomogeneity

The infrared transmission spectra for all samples are shown in Fig. 1. For normal spinel-type compounds, unit-cell

TABLE I. Fitting parameters for $\text{FeCr}_{2-x}\text{Al}_x\text{S}_4$.

x	0.1	0.2	0.4	0.5	0.6	0.7	0.8	1.0
d (Å)	9.9912	9.9997	10.0006	9.9949	9.9997	10.0047	10.013	10.000
T_c (K)	167	157	139	129	120	115		
E_L (meV)	22	31.5	34.5	38.7	36.9	41.5	41	VRH
E_p (meV)	138	152	172	154	152	153	VRH	VRH

group analysis predicts that there are four infrared active vibrations of F_{1u} modes.¹⁴ In our detecting frequency range, only one infrared absorption peak is observed for each sample, which is responsible for the $F_{1u}(1)$ mode.^{15,16} As seen from Fig. 1, the absorption peak shifts to higher frequency gradually with the increase of x . The systematic variation of the absorption peak on substitution of Cr by Al clearly indicates that Al atoms get into lattice. More important is that the absorption peak shifts to high frequency, which reveals that the bond strength of the Al-S bond is stronger than that of the Cr-S bond, and it may be further deduced that Al ions have a different Coulomb potential in contrast to Cr ions. Thus it can be concluded that Al substitution induces the fluctuation.

In addition, since the Al ion is nonmagnetic, the substitution of Cr by Al ions will cause not only the fluctuation but also magnetic inhomogeneity in the Cr sublattice. As is known, the magnetism of the Cr sublattice and that of the Fe sublattice couples with each other. Thus the magnetic inhomogeneity in the Cr sublattice will also induce the magnetic inhomogeneity in the Fe sublattice. Because the conduction in FeCr_2S_4 is originated from the Fe^{2+} narrow band, the magnetic inhomogeneity in the Fe sublattice will inevitably influence the transport behavior. So we have studied the magnetism of $\text{FeCr}_{2-x}\text{Al}_x\text{S}_4$.

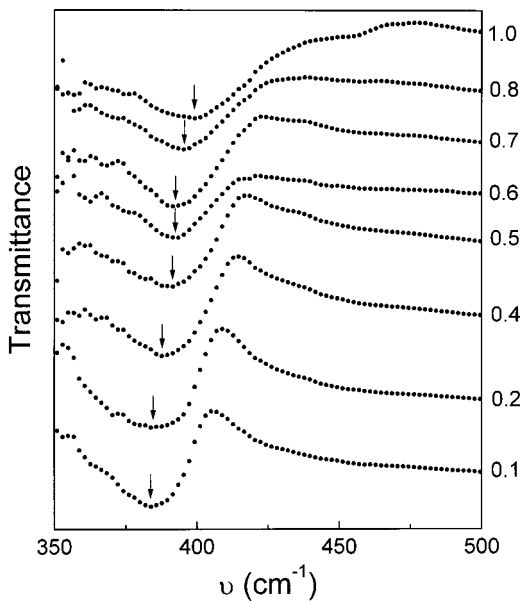


FIG. 1. Infrared transmission spectra for $\text{FeCr}_{2-x}\text{Al}_x\text{S}_4$ ($0 < x \leq 1.0$) samples.

C. Macromagnetism

The magnetization as a function of temperature for the samples with $x \leq 0.7$ is plotted in Fig. 2. It can be seen that all the samples undergo a transition from paramagnetic to ferrimagnetic phase. The Curie temperature T_c , derivative of $M(T)$, decreases with the increase of x (as shown in Table I). On substitution of Al for Cr the magnetic transition weakens and broadens and the magnitude of magnetization decreases. In $\text{FeCr}_{2-x}\text{Al}_x\text{S}_4$, as is known, because the Al ion is nonmagnetic, the magnetism of the Cr sublattice will decrease with increasing x . For a certain substituting concentration, the net magnetism of the system may be negative. Thus for $x=0.8$ and 1.0 , in order to obtain the intrinsic magnetism of the system, we performed the low-field magnetization measurement (measuring magnetic field 0.005 T). The M - T curves for $x=0.8$ and 1.0 are shown in Fig. 3(a). With decreasing temperature, the magnetization first rises to a maximum then decreases to zero at a compensation temperature. The compensation temperature is 25 and 40 K for $x=0.8$ and 1.0 , respectively. With further decreasing temperature, the net magnetization below the compensation temperature is negative.

As is known, the compensation temperature is a characteristic of ferrimagnets, which was first predicted by Néel and then discovered in some ferrimagnets.^{17,18} The magnetic structure in FeCr_2S_4 has been investigated long ago by the

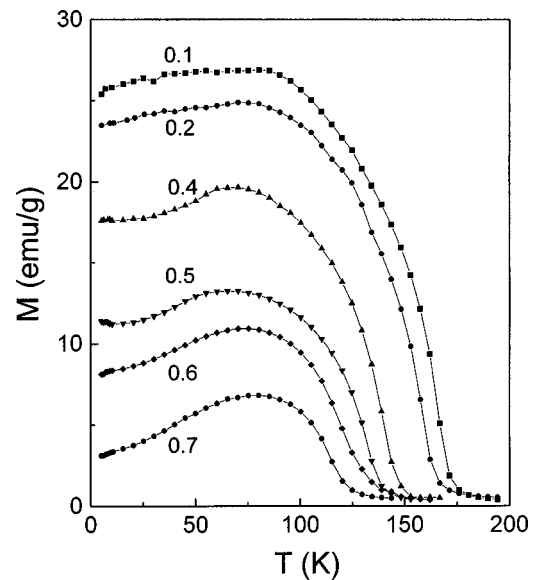


FIG. 2. Temperature dependence of the magnetization ($M \sim T$) for $\text{FeCr}_{2-x}\text{Al}_x\text{S}_4$ ($0 < x \leq 0.7$) samples.

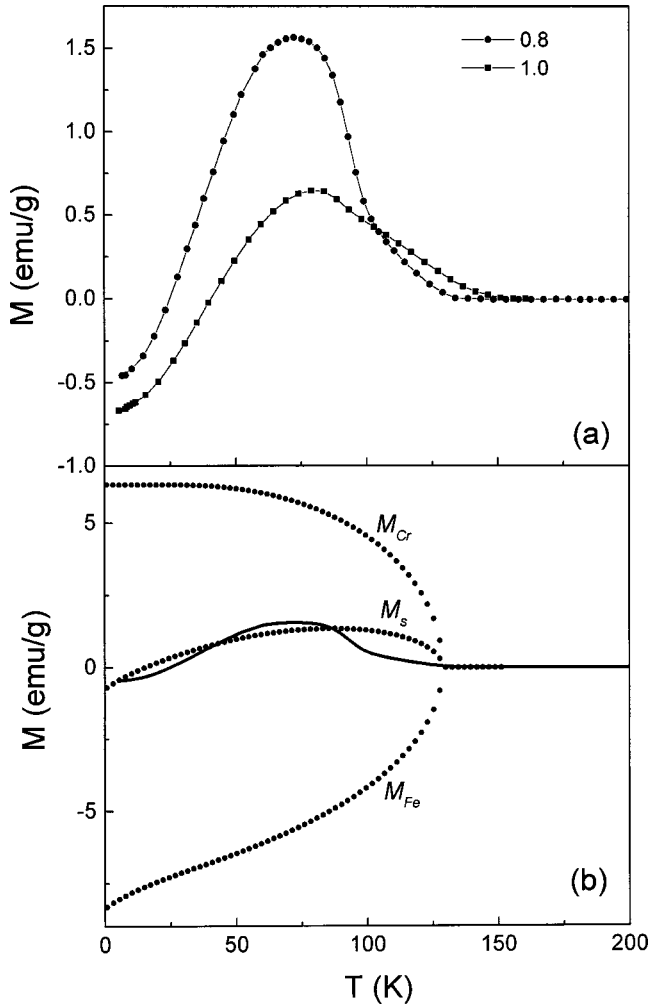


FIG. 3. (a). Temperature dependence of the low-field magnetization ($M \sim T$) for $x \geq 0.8$. (b). Solid line is the experimental result of magnetization for $x=0.8$, three dotted lines are the theory results of formula (1).

powder neutron-diffraction technique, which showed that the spin arrangement in FeCr_2S_4 is simple Néel type with $\mu_{\text{Cr}} = 2.9\mu_B$ and $\mu_{\text{Fe}} = 4.2\mu_B$, the magnetic moment of the Cr ion is in the direction of applied field, and the magnetic moment of the Fe ion is in a direction opposite to that of the applied field.¹⁹ Then according to Néel's two-sublattice model, for FeCr_2S_4 , both the Fe sublattice and the Cr sublattice are ferromagnetic, while the magnetic moment of the Fe sublattice is antiparallel to that of the Cr sublattice due to the magnetic coupling between these two sublattices. Thus the net magnetization M_s can be written as¹⁸

$$M_s = M_{\text{Cr}} - M_{\text{Fe}} \quad (1)$$

where M_{Fe} and M_{Cr} are the spontaneous magnetizations of the Fe and Cr sublattices, respectively. For $\text{FeCr}_{2-x}\text{Al}_x\text{S}_4$, M_{Cr} and M_{Fe} can be written as

$$M_{\text{Cr}} = (2-x)Ng_{\text{Cr}}J_{\text{Cr}}\mu_B B_{J_{\text{Cr}}}(y_{\text{Cr}}),$$

$$M_{\text{Fe}} = Ng_{\text{Fe}}J_{\text{Fe}}\mu_B B_{J_{\text{Fe}}}(y_{\text{Fe}}),$$

$$y_{\text{Cr}} = g_{\text{Cr}}J_{\text{Cr}}\mu_B H_{\text{Cr}}/kt,$$

$$y_{\text{Fe}} = g_{\text{Fe}}J_{\text{Fe}}\mu_B H_{\text{Fe}}/kt,$$

where H_{Cr} and H_{Fe} are the total molecular fields acting on Fe and Cr ions, respectively.

$$H_{\text{Cr}} = H_0 + \gamma_{\text{FeCr}}(-M_{\text{Fe}} + \beta M_{\text{Cr}}), \quad (1a)$$

$$H_{\text{Fe}} = H_0 + \gamma_{\text{FeCr}}(\alpha M_{\text{Fe}} - M_{\text{Cr}}), \quad (1b)$$

where α , β , and γ_{FeCr} are the molecular-field coefficients.

In FeCr_2S_4 , because the magnetic moment of the Cr sublattice is larger than that of the Fe sublattice, it can be expected that the system displays a net positive magnetization at temperatures below T_c . Clearly, with increasing x , the spontaneous magnetization of the Cr sublattice M_{Cr} decreases, thus M_s decreases. The substitution of Al for Cr has two influences to the magnetism, one is that the substitution of nonmagnetic Al ions will destroy the magnetism of the Cr sublattice, which causes the weakening of magnetic coupling between two sublattices. The other is that the Coulomb-potential fluctuation of Al ions will induce the random fluctuation of the spins in the Cr sublattice, and the fluctuation of the spins in the Cr sublattice can only be depressed at lower temperatures. Thus T_c reduces, the magnetic transition broadens and weakens (as seen from Fig. 2). The magnetism of the Cr sublattice decreases with further increasing Al content, then at $x=0.8$ and 1.0 , the compensation effect occurs. The comparison of the experimental result for $x=0.8$ with formula (1) is shown in Fig. 3(b). Clearly, the theory accords with the experimental result qualitatively. Because of the substitution of high-concentration aluminum, the magnetism of the Cr sublattice decreases. As seen from Fig. 3(b), at temperatures below the compensation temperature, $M_{\text{Cr}} < M_{\text{Fe}}$. At higher temperatures (from about 90 to 130 K), the experimental value is less than the theoretical value, this just indicates that the paramagnetic-ferrimagnetic transition takes place in this temperature range. Theoretically, the compensation effect should occur in the sample with x around 0.55 if the magnetism of the Fe sublattice is not destroyed ($\mu_{\text{Fe}} \approx 1.45\mu_{\text{Cr}}$). The compensation effect taking place in higher doping samples indicates clearly that the magnetism of the Fe sublattice weakens either.

D. Micromagnetism

The macromagnetism deduced above should also be reflected in micromagnetism of the system. Here we further investigated the micromagnetism by the ESR. Figure 4 shows the temperature dependence of the ESR signal for the samples with $x=0.2, 0.4, 0.6, 0.8$, and 1.0 . Since the ESR spectra for FeCr_2S_4 sample have already been debated elsewhere,¹¹ below we are only concerned with the variation of the spectra with Al substituting. For FeCr_2S_4 , as seen from the ESR spectra in our previous work,¹¹ only one ESR signal is observed with the g -factor near 2 at temperatures above T_c . The ESR spectrum splits at 155 K, and the splitting peaks shift towards lower and higher fields with decreasing temperature, respectively. The ESR spectra for the x

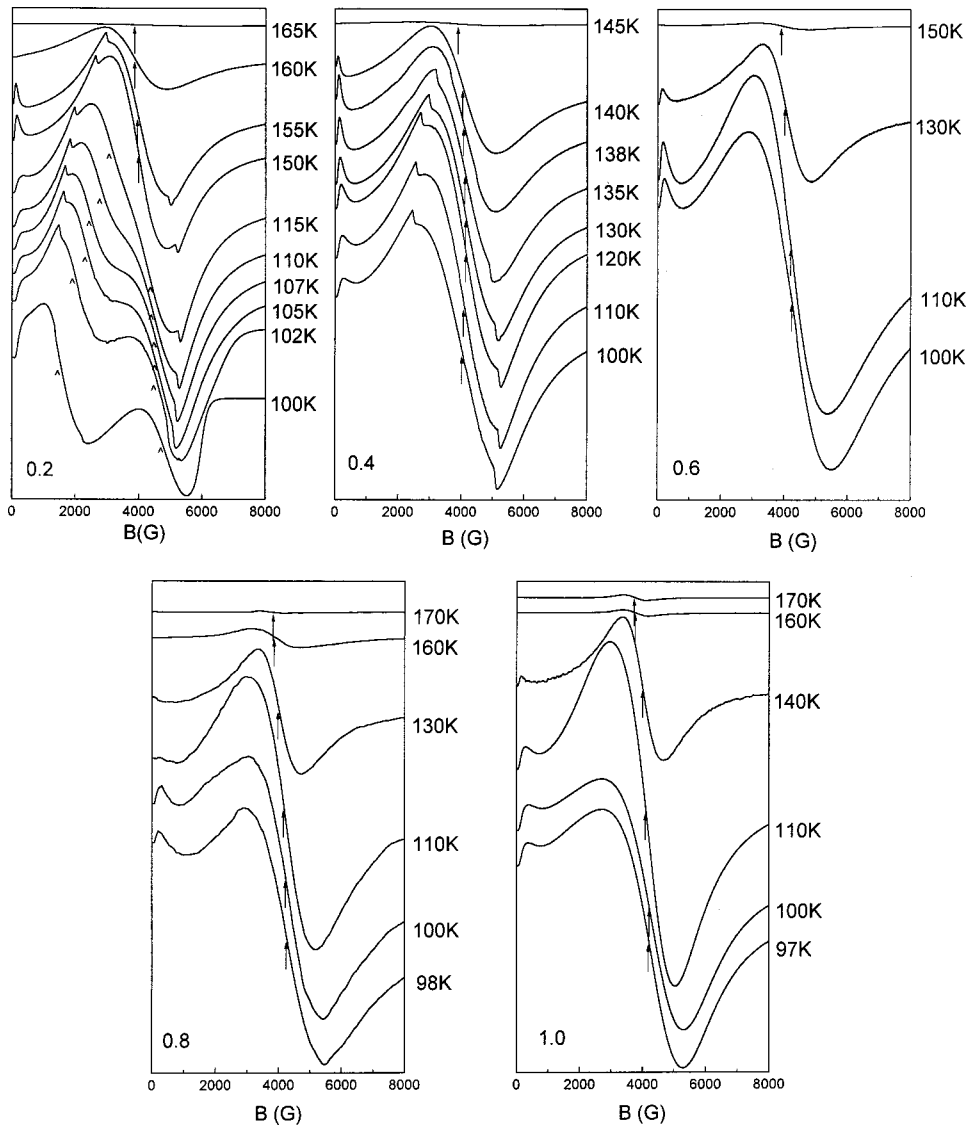


FIG. 4. ESR spectra at different temperatures for $\text{FeCr}_{2-x}\text{Al}_x\text{S}_4$ ($x=0.2, 0.4, 0.6, 0.8,$ and 1.0) samples. Dark arrow marks the single signal, “ \wedge ” marks the splitting peaks.

$x=0.2$ sample are similar to that for FeCr_2S_4 , however, the splitting peaks emerge at lower temperatures (below 115 K). For $x \geq 0.4$, only a single ESR signal is observed in the measured temperature range. It must be noted that for the Al-substituting sample, even if for a lower concentration with $x=0.2$, the ESR resonance line locates at a higher field. With increasing x , the ESR line is broadened.

For FeCr_2S_4 , the splitting peaks are believed to result from the antiparallel magnetic arrangement between the Fe sublattice and the Cr sublattice.¹¹ The moment of the Cr sublattice is susceptible to be parallel to the applied field, hence the internal field of the Cr sublattice may cause its ferromagnetic-resonance line shift to lower fields, which forms the left-branch signal. So does the Fe sublattice, while it is antiparallel and causes the right-branch signal. From formulas (1a) and (1b), it is known that the field acting on Cr (or Fe) ions consists of three parts: the internal field of the Cr (Fe) sublattice acting on Cr (Fe) ions, the internal field of the Fe (Cr) sublattice acting on Cr (Fe) ions, and the applied field. For lower-concentration aluminum sample, the internal field of the Cr sublattice is larger than that of the Fe sublat-

tice, thus the net internal field is in the direction of the applied field and the ESR signal of Cr ions occurs at lower fields (below 0.34 T). With increasing x , the magnetism of the Cr sublattice decreases and the internal field acting on Cr ions weakens. Thus the resonance line of Cr ions shifts to higher fields and the splitting signal for $x=0.2$ emerges at lower temperature. With further increasing x , the resonance line of Cr ions shifting further to higher field merges into the right-branch signal. As a whole, the ESR signal behaves as a single line. When x is large, the net field is negative, thus the net field acting on Cr ions is antiparallel to the applied field, as a result ESR resonance takes place at fields higher than 0.34 T.

Also as the substitution of Al for Cr divides the Cr sublattice into a number of domains with short-range order, this will inevitably induce magnetic inhomogeneity to system, that is to say, a certain number of relatively magnetic strong regions and magnetic weak regions in the Cr sublattice may form. These magnetic strong and weak regions in the Cr sublattice will result in the corresponding strong and weak regions in the Fe sublattice because of the coupling between

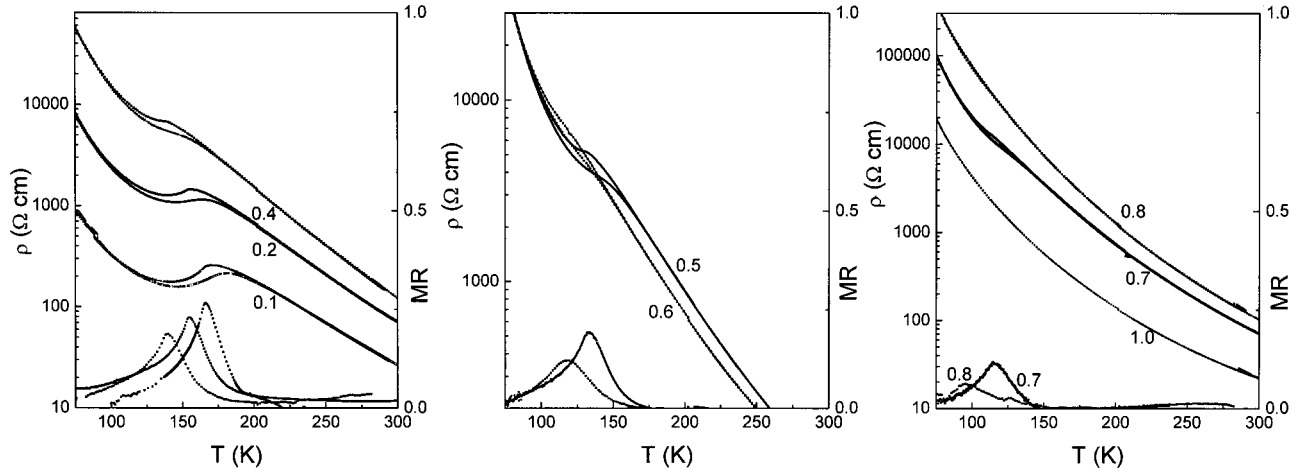


FIG. 5. Resistivity, ρ , and magnetoresistance $MR_H = [\rho(0) - \rho(H)]/\rho(0)$, versus temperature for $\text{FeCr}_{2-x}\text{Al}_x\text{S}_4$ ($0 < x \leq 1.0$).

the two sublattices, which will also induce magnetic inhomogeneity. The magnetic inhomogeneity is just the reason for the broadening of the ESR spectrum.

From ESR and magnetization, it can be concluded that the substitution of Al for Cr destroys not only the magnetism of the Cr sublattice but also the magnetism of the Fe sublattice. Thus it can also be deduced that Al substituting induces the magnetic fluctuations to the system. The magnetic fluctuations as well as the Coulomb fluctuations in the system will inevitably influence the transport behavior, then we performed the resistivity measurements.

E. The conductivity from magnetic polarons to VRH process

The resistivity ρ and magnetoresistance $MR_H = [\rho(0) - \rho(H)]/\rho(0)$, as a function of temperature are shown in Fig. 5. Comparing with FeCr_2S_4 , the Al-contained sample has a higher zero-field resistivity. For lower aluminum concentration ($0 < x \leq 0.2$), both ρ and MR_H display a peak near T_c . For $0.4 \leq x \leq 0.7$, the resistivity has no peak, however it is clear that the resistivity shows a point of inflection near T_c and the CMR effect occurs in that temperature range. The point of inflection in the resistivity curve becomes less clear with increasing Al content and disappears when $x \geq 0.8$. For the $x = 1.0$ sample, the resistivity displays a semiconductor-like behavior in the whole temperature range measured, and no appreciable CMR effect is observed.

As is known, for semiconductorlike transport behavior, there are three models. (1) An Arrhenius law, $\rho = \rho_0 \exp(E/k_B T)$, is generally used to model activated behavior due to a band gap E or a mobility edge. (2) Nearest-neighbor hopping of small polarons, $\rho = \rho_0 T \exp(E_p/k_B T)$. (3) If the carriers are localized by random potential fluctuations, Mott's VRH expression $\rho = \rho_0 \exp(T_0/T)^{1/4}$ is appropriate.²⁰⁻²² Thus in order to understand the transport mechanism in the FeCr_2S_4 system, it is necessary to fit the resistivity curves based on these three descriptions. Figure 6 shows the zero-field resistivity curves replotted as $\ln \rho - 1000/T$, $\ln(\rho/T) - 1000/T$, and $\ln \rho - (1000/T)^{1/4}$, respectively. For the sample with $x = 0.1$, as seen from Fig. 6, the curve of $\ln \rho$ versus $1000/T$ is linear both at $T > T_c$ and at

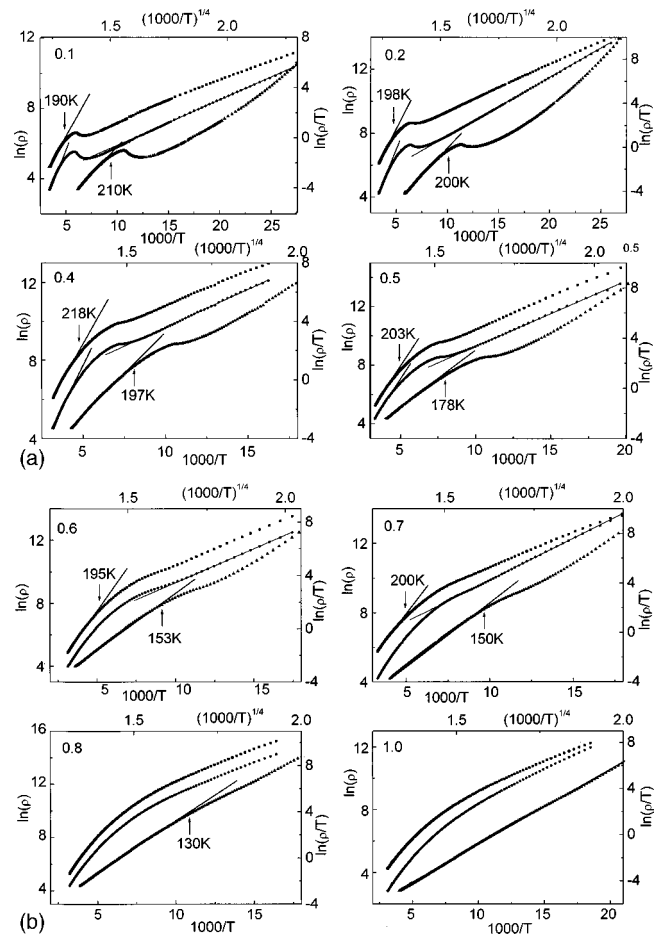


FIG. 6. Zero-field resistivity curves for $\text{FeCr}_{2-x}\text{Al}_x\text{S}_4$ ($0 < x \leq 1.0$) replotted as $\ln \rho - 1000/T$ (closed circle \bullet), $\ln(\rho/T) - 1000/T$ (solid square \blacksquare), and $\ln \rho - (1000/T)^{1/4}$ (up triangle \blacktriangle), respectively. The solid lines are the linear fitting curves, the temperature value shown in the figure marks the temperature where the experimental curve deviates from linearity.

temperature far below T_c , indicating a semiconductorlike behavior in two regions. The activation energy E obtained from the fits to $\rho = \rho_0 \exp(E/k_B T)$ reads $E_H = 118$ meV and $E_L = 22$ meV, respectively. In our previous work, the discrepancy between E_L and E_H for FeCr_2S_4 has been discussed in detail and been attributed to magnetic-polaron conduction.¹¹ As we know, a magnetic polaron is a carrier coupled by short-range magnetic correlation within a magnetic cluster at temperatures above T_c . Accordingly, the effective mass of a magnetic polaron increases greatly with respect to that of a naked carrier, therefore the magnetic polaron has a lower mobility and a higher activated energy. The formation of a magnetic polaron will become impossible if the system is in an ideal ferromagnetic or ferrimagnetic order, this explains the rapid fall off in resistivity observed near T_c . Likewise, an external magnetic field will increase the magnetic order and inhibit the formation of the magnetic polaron, thus CMR occurs.^{20,23,24} As seen from Fig. 6, for the samples with $0 < x \leq 0.2$, the resistivity can be described by thermal-activated conduction [$\rho = \rho_0 \exp(E/k_B T)$] at low-temperature range, and can be better fitted by magnetic-polaron hopping conduction [$\rho = \rho_0 T \exp(E_P/k_B T)$] at high-temperature range, respectively. The activated energies E_L and E_P obtained from each fit are listed in Table I. Clearly, E_P increases with Al content. In the middle concentration with $0.4 \leq x \leq 0.7$, the resistivity at temperatures above T_c could be better fitted by the VRH expression. For the samples with $x \geq 0.8$, the resistivity could be well described by VRH in the whole temperature range measured. All the results clearly suggest that the transport mechanism transits from magnetic-polaron transport to VRH with the increase of

Al content. As mentioned above, Al substitution divides the system into a number of magnetic clusters and induces spatial fluctuations in both the Coulomb and magnetic potentials, which increases the magnetic scattering and favors the carrier localization. Thus the resistivity increases. With increasing Al content, the carrier becomes more localized and the activation energy becomes larger, then the nearest-neighbor hopping process with a high activation energy may transform into uncorrelated VRH when the available phonon energy is so small as to make the longer-range hops necessary to find a site sufficiently close in energy for hopping to occur.²⁵ Furthermore, as shown in Fig. 2, the magnetic transition weakens and broadens with increasing x . As a consequence, with increasing Al content, the CMR effect decreases gradually and disappears at last.

IV. CONCLUSION

In conclusion, the magnetic and transport properties of $\text{FeCr}_{2-x}\text{Al}_x\text{S}_4$ ($0 < x \leq 1.0$) are studied. The experimental results of infrared spectra and ESR indicate clearly that Al substituting induces both Coulomb- and magnetic-potential fluctuations, which favor carrier localization. With increasing Al content, the transport behavior transits from the magnetic-polaron conduction into the VRH process.

ACKNOWLEDGMENTS

This work was supported by the National Natural Science Foundation of China and the Foundation of Academia sinica, People's Republic of China, as well as the Research Fund for the Doctoral Program of Higher Education.

*Corresponding author. FAX: 86-551-3602803. Email address: yzr@mail.ustc.edu.cn

¹K. Chahara, T. Ohno, M. Kassai, and Y. Kozono, *Appl. Phys. Lett.* **63**, 1990 (1993).

²R. Von Helmolt, J. Wecker, B. Holzapfel, L. Schultz, and K. Samwer, *Phys. Rev. Lett.* **71**, 2331 (1993).

³S. Jin, T. H. Tiefel, M. McCormack, R. A. Fastnacht, R. Ramesh, and J. H. Chen, *Science* **264**, 413 (1994).

⁴C. Zener, *Phys. Rev.* **82**, 403 (1951).

⁵A. J. Millis, P. M. Littlewood, and B. I. Shraiman, *Phys. Rev. Lett.* **74**, 5144 (1995).

⁶J. M. D. Coey, M. Viret, L. Ranno, and K. Ounadjela, *Phys. Rev. Lett.* **75**, 3910 (1995).

⁷M. Ziese and C. Srinivawarawong, *Phys. Rev. B* **58**, 11 519 (1998).

⁸A. P. Ramirez, R. J. Cava, and J. Krajewski, *Nature (London)* **386**, 156 (1997).

⁹Z. W. Chen, S. Tan, Z. R. Yang, and Y. H. Zhang, *Phys. Rev. B* **59**, 11 172 (1999).

¹⁰J. B. Goodenough, *J. Phys. Chem. Solids* **30**, 261 (1969).

¹¹Z. R. Yang, S. Tan, Z. W. Chen, and Y. H. Zhang, *Phys. Rev. B* **62**, 13 872 (2000).

¹²P. Gibart, M. Robbins, and V. G. Lambrecht, *J. Phys. Chem. Solids* **34**, 1363 (1973).

¹³P. K. Baltzer, P. J. Wojtowicz, M. Robbins, and E. Lopatin, *Phys. Rev.* **151**, 357 (1966).

¹⁴W. K. Unger, B. Farnworth, J. C. Irwin, and H. Pink, *Solid State Commun.* **25**, 913 (1978).

¹⁵H. D. Lutz, W. Becker, B. Müller, and M. Jung, *J. Raman Spectrosc.* **20**, 99 (1989).

¹⁶E. Riedel and T. Dützmänn, *Mater. Res. Bull.* **16**, 65 (1981).

¹⁷N. Menyuk, K. Dwight, and D. G. Wickham, *Phys. Rev. Lett.* **4**, 119 (1960).

¹⁸L. Néel, *Ann. Phys. (Paris)* **3**, 137 (1948).

¹⁹G. Shirane, D. E. Cox, and S. J. Pickart, *J. Appl. Phys.* **35**, 954 (1964).

²⁰R. M. Kusters, J. Singleton, D. A. Keen, R. McGreevy, and W. Hayes, *Physica B* **155**, 362 (1989).

²¹M. Viret, L. Ranno, and J. M. D. Coey, *Phys. Rev. B* **55**, 8067 (1997).

²²G. J. Snyder, R. Hiskes, S. Dicarolis, M. R. Beasley, and T. H. Geballe, *Phys. Rev. B* **53**, 14 434 (1996).

²³Mark Rubinstein, D. J. Gillespie, John E. Snyder, and Terry M. Tritt, *Phys. Rev. B* **56**, 5412 (1997).

²⁴Y. Shapira, S. Foner, N. F. Oliveira, and T. B. Reed, *Phys. Rev. B* **10**, 4765 (1974).

²⁵J. M. D. Coey, *Philos. Trans. R. Soc. London, Ser. A* **356**, 1519 (1998).